Applied Nanoscience
https://doi.org/10.1007/s13204-020-01284-3

ORIGINAL ARTICLE

Antitumor activity of spherical nanoparticles $GdYVO_4:Eu^{3+}$ depends on pre-incubation time

Anatoliy M. Goltsev[1] · Yuriy V. Malyukin[2] · Natalya M. Babenko[1] · Yulia O. Gaevska[1] · Mykola O. Bondarovych[1] · Tatiana G. Dubrava[1] · Igor F. Kovalenko[1] · Maksym V. Ostankov[1] · Vladimir K. Klochkov[2]

Received: 14 December 2018 / Accepted: 10 February 2020

Abstract

The significance of tumor cells incubation with spherical nanoparticles based on orthovanadates of rare-earth elements activated by europium $GdYVO_4:Eu^{3+}$ in the effectiveness of Ehrlich carcinoma growth inhibition was shown. Ehrlich carcinoma cells were incubated with nanoparticles for 1, 2, 3, and 4 h; afterwards, their accumulation in cells using a LSM 510 META confocal laser microscope (Carl Zeiss, Germany), changes in mitochondrial function and apoptotic/necrotic cells were assessed. Even from the 1st hour of incubation, there was observed an increase in mean fluorescence intensity, indicating the beginning of nanoparticles accumulation inside the cells. By the third hour of incubation, the fluorescence values of total Ehrlich carcinoma population reached the maximum values. At the same time, the appearance of single cells with ultra-high level of fluorescence was established; the number of those did not exceed 5%. By the third hour of incubation with nanoparticles, there was a significant mitochondrial dysfunction of Ehrlich carcinoma cells and a convincing increase in the proportion of cells in the late apoptosis (An^+/PI^+) and necrosis (An^-/PI^+) compared to the control. The aforesaid changes in the Ehrlich carcinoma cells after 3-h pretreatment with nanoparticles contributed to the highest decrease in intensity of tumor growth in vivo down to 41.80%. Thus, the successful implementation of an antitumor effect of nanoparticles based on orthovanadates of rare earth elements activated by europium $GdYVO_4:Eu^{3+}$ implies their penetration and accumulation inside the cells as well as associated with impaired mitochondrial function and induction of apoptotic and necrotic changes in tumor cells.

Keywords Cancer · Ehrlich carcinoma cells · Nanoparticles · Confocal microscopy

Introduction

Recently, the methods of nanobiotechnology have been applied in the revealing, diagnosis and treatment of cancer and this application led to the emerging new scientific direction, nanooncology. There is a general tendency to create multifunctional nanocomposites, combining diagnostic and therapeutic features, which is one of the main tasks of theranostics. It is assumed that vanadium derivatives, in particular, nanoparticles (NPs) of gadolinium orthovanadates activated by europium, are capable of solving such tasks, since they simultaneously possess an antitumor activity and ability to fluorescence. Their unique luminescent properties, such as narrow spectral lines with high Stokes shift, high quantum yield, no flickering effect, high photostability, allow them to be used as luminescent probes in biological studies for tagging and long-term monitoring of the state of biological objects in vivo (Klochkov et al. 2013). Previously, we reported about the ability of rare-earth orthovanadates and hybrid nanocomplexes based on them, containing cholesterol, to visualize in vitro cancer stem cells of Ehrlich carcinoma (EC) (Goltsev et al. 2013; Goltsev et al. 2016). In these studies, the intracellular accumulation of NPs in the EC cells was confirmed using the method of spectral analysis. However, the question of the predominant accumulation of the used NPs in a particular the cellular compartment (nucleus, cytoplasm) remains unclear. The

✉ Anatoliy M. Goltsev
cryopato@gmail.com

[1] Institute for Problems of Cryobiology and Cryomedicine, National Academy of Sciences of Ukraine, Pereyaslavska Str. 23, Kharkiv 61016, Ukraine

[2] Institute for Scintillation Materials, National Academy of Sciences of Ukraine, 60 Nauki Ave., Kharkiv 61001, Ukraine

Published online: 02 March 2020

answer to this question will enable to get closer to understanding the mechanism for the implementation of their antitumor influence.

A convenient tool for solving this experimental problem is the method of confocal microscopy. The use of a multispectral mode of a laser scanning microscope makes it possible to investigate the spatial interposition in the cell of the substances capable of fluorescence, in particular, NPs. Investigating these preparations in a fluorescent microscope, one cannot assert with certainty that the NPs are on the surface of the cell or inside it. Using the method of optical sections and further 3D reconstruction of the object, it is possible to reproduce the volume distribution of the NPs in a cell, as well as to evaluate the research results in four dimensions: length, width, depth and time (LSM and LSM 510 2005).

The possibility of using the NPs in the targeted cancer therapy is based on the existence of the effect of "enhanced permeability and retention". The general explanation of this phenomenon consists in the fact that an active proliferation of tumor cells stimulates an enhanced angiogenesis of the tumor site by increasing the production of vascular endothelial growth factor and other growth factors. Newly formed tumor vessels are usually abnormal in shape and architecture, i.e., they do not have a smooth muscle layer, the endothelial cells lining them have wide gaps, etc. In addition, the tumor tissues usually lack effective lymphatic drainage. All these factors lead to an abnormal dynamics of the transfer of molecules and liquids, allowing the NPs or nanocontainers with therapeutic drugs to selectively penetrate and be accumulated inside the tumor, reducing the severity of the side effects associated with traditional methods of treatment.

The antitumor activity of orthovanadates and other vanadium compounds has now been proven both in clinic and in experiment. Its advantages include a low IC50 (half maximal inhibitory concentration) (Rozzo et al. 2017), the presence of an antiproliferative and proapoptotic effect on malignant melanoma cell lines. In the reports (Dabros et al. 2004), the antitumor effect of some organic derivatives of vanadium [V (IV)] (bis-(maltolato) oxovanadium (IV), bis- (coyato) oxovanadium (IV) and bis 2,2′-bipyridine) oxovanadium (IV) sulfate) was demonstrated, the addition of which to the culture of the H-35 tumor cells at a 0.5–5.0 mM concentration led to a significant inhibition of its growth and proliferation. Vanadyl sulfate [V (IV)] or vanadate [V (V)] had a similar effect on tumor cells (Kordowiak et al. 2007).

Vanadium compounds are capable of causing the selective oxidation of pyrimidine bases, which prevent the complementary strand of DNA (Rodríguez-Mercado et al. 2011). This is particularly susceptible to tumor cells, which are characterized by disorders in the DNA repair system. Another supposed mechanism of the antitumor action of vanadium compounds is the disturbance of the permeability of mitochondrial membrane of tumor cells caused by them due to the generation of reactive oxygen species (Molinuevo et al. 2004), which leads to the release of cytochrome C and apoptosis induction (Korbecki et al. 2012).

In experimental studies aimed at investigations of the effect of various factors and therapeutic agents directly on a functional activity of cancer cells, the ascitic form of EC, being a line of undifferentiated mouse cancer cells, inoculated in vivo, can be used (Ozaslan et al. 2011).

In our previous studies, demonstrating the EC growth inhibition under the effect of NPs of rare-earth orthovanadates (Goltsev et al. 2017; Goltsev et al. 2015), the incubation of cells with nanomaterials was suggested to be important in manifestation of such an effect. However, the incubation period in these studies was selected according to the data obtained in liver cells (Klochkov et al. 2013).

The purpose of this study was to determine the optimal time for incubation of tumor cells with NPs, leading to effective inhibition of tumor growth.

Materials and methods

Obtaining EC cells in vivo

Ehrlich carcinoma (EC) cells were grown in peritoneal cavity (PC) of 8-month-old female Balb/C mice. Inoculation was performed in the left lower quadrant of the abdominal wall. The EC cells cryopreserved in ascitic fluid (Holtsev et al. 2011), stored at the Low-Temperature Bank of the Institute for Problems of Cryobiology and Cryomedicine of the National Academy of Sciences of Ukraine at − 196 °C, were used as a primary culture. After warming, the EC cells were inoculated three times in vivo in order that they acquire the morphological and functional signs of native (not subjected to freezing) cells (Goltsev et al. 2012).

The EC cells stabilized in such a way were intraperitoneally administered at a dose of 3×10^6 cells/mouse in 0.3 ml of saline and cultured for 7 days in vivo; then the animals were removed from the experiment under light ether anesthesia. The EC cells were obtained from PC with a syringe, which was pre-washed with sterile saline with heparin, with a thick needle No. 10 of 2.69-mm inner diameter. Indices of the EC cells, obtained as above mentioned in future, were assumed as a control.

Obtaining nanoparticles

Spherical nanoparticles (NPs) based on orthovanadates of rare earth elements (Gd, Y) activated by europium $GdYVO_4:Eu^{3+}$ (1.3 g/l), synthesized at the Institute for Scintillation Materials of the National Academy of Sciences of Ukraine, were used in the research.

Chlorides of rare earth elements (99.9%), sodium citrate $Na_3C_6H_5O_7{\cdot}2H_2O$ (> 99%) and anhydrous sodium metavanadate (96%) were obtained from Acros organics (USA). Sodium hydroxide (99%) was purchased from JSC Macrokhem (Ukraine). Sodium orthovanadate Na_3VO_4 solution was obtained by adding a 1-M solution of NaOH in aqueous solution $NaVO_3$ to pH 13. Particle morphology and size distribution were analyzed using Transmission Electron Microscopy. Samples were prepared by placing a drop of a colloidal solution onto a 200-mesh holey carbon copper grid. The grid was air dried under dust-free conditions and examined in TEM 125 K (JSC, Ukraine) electron microscope at 100-kV electron beam. The size of NPs in colloidal solutions before and after addition of the dyes was determined by dynamic light scattering (DLS). The hydrodynamic diameter and ζ-potential of nanoparticles were measured with a ZetaPALS analyzer (Brookhaven Instruments Corp., USA). Before the measurements, the test solutions were incubated at 25 °C. Colloidal solutions containing spherical particles were prepared by the method described earlier using sodium citrate as a stabilizing agent (Klochkov 2009). At this stage of the synthesis, lanthanide chelator makes its contribution to the slow formation of a heterogeneous system as thermal degradation of the complex. On the other hand, citrate molecules, forming chelate complexes with cations on the surface of the solid phase, form protective layers, preventing coagulation of the colloidal system. Briefly, 10 mL of aqueous solution of rare-earth chlorides (0.01 mol/L) was mixed with 8 mL of sodium citrate solution (0.01 mol/L). Then, the obtained solution 8-mL Na_3VO_4 (0.01 mol/L) was flowed drop by drop (pH 13). The mixture was intensively stirred using a magnetic stirrer until yellowish transparent solution is formed. The solution was heated on a water bath for 30 min till 24 h at 90 or 100 °C. According to the TEM, solid phase of colloidal solution represents spherical NPs with average size of 2 ± 0.2 nm. Through DLS measurements, the average volume-weighted hydrodynamic diameter of NPs was determined to be 8.5 nm (Fig. 1). The average value of ζ-potential was -36 ± 2 mV. The solutions were purified by dialysis with 'Cellu Sep H1' 3.5 kDa membrane. The solution is transparent in transmitted light and opalescent in lateral light (Tyndall cone). Colloidal particles pass easily through nitrocellulose ultrafilters with a pore diameter of 100 nm. The solid phase concentration is 1 g/L. pH is 7.4–7.6. The solutions were stored in sealed ampoules without changing their properties for more than 2 months at normal conditions.

Pretreatment of EC cells with nanoparticles

The EC cells were incubated with NPs in a 5% glucose solution at room temperature for 1, 2, 3, and 4 h. Below these groups will be called as "experimental". Then the cells were washed three times with 5% glucose solution by gentle centrifugation. The control cells were the EC ones, incubated in a solution of 5% glucose without the NPs. Number of EC cells after the incubation period was counted in the Goryaev chamber.

The EC cell viability was assessed by supravital trypan blue staining (Trypan blue solution, Sigma, USA) and taking into account the number of cells with a disordered integrity of the cell membrane, which was evaluated as unviable.

Mitochondrial activity as a function of viable cells was assessed using the cell growth determination kit MTT (Stock No. CGD-1, Sigma, USA) according to the manufacturer's instructions. Afterwards, the MTT, dimethylthiazole-diphenyltetrazoliumbromide reagent, was added to the cell culture ($1x10^6$ cells) at a concentration of 5 mg/ml and incubated for 3 h at 37 °C. Next, MTT solvent was added to the cells, pipetted thoroughly and kept for another 15 min at room temperature. The results were detected by measuring the optical density of the samples using a spectrophotometer (SF-46 "LOMO") at a 560-nm wavelength.

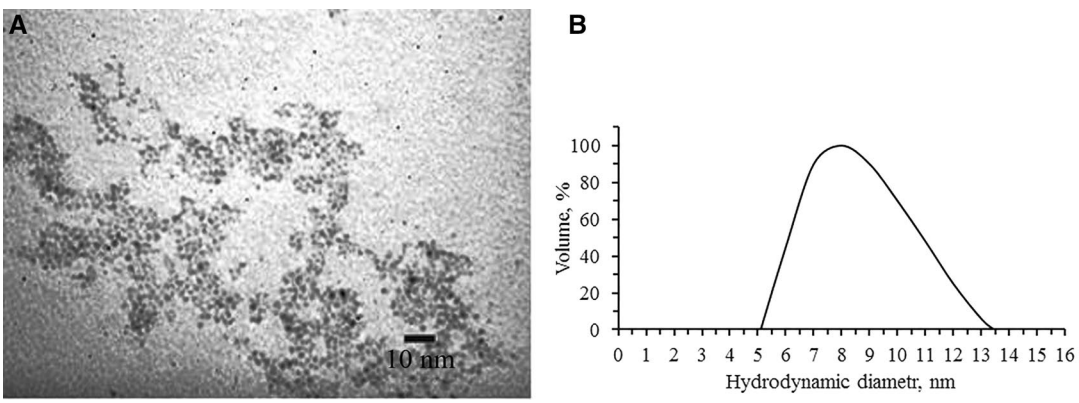

Fig. 1 TEM image of nanoparticles $GdYVO_4:Eu^{3+}$ (**a**) and their hydrodynamic diameter through DLS measurements (**b**)

Identification of apoptotic and necrotic cells

At the end of incubation period, the EC cells with NPs were precipitated by centrifugation, resuspended in cold PBS (4 °C). The processes of necrosis/apoptosis were studied with Annexin-V (BD, USA, Cat. # 556419) and propidium iodide—PI (Sigma, USA, Cat. # 81845-25MG) dyes using FACS Calibur Becton–Dickinson flow cytometer. The proportion of living cells (Annexin V^-/PI^-), apoptotic cells (Annexin V^+/PI^-), necrotic cells (Annexin V^-/PI^+) and cells in a state of post apoptotic necrosis (Annexin V^+/PI^+) was determined.

Identification of NPs in EC cells

The number of cells bound to NPs was counted using an LSM 510 META confocal laser scanning microscope (Carl Zeiss, Germany). For the excitation of fluorescence, a diode laser with a wavelength of 405 nm and a power of 10 mW was used. To observe fluorescence, an emission filter was used for NPs 583–636 nm. An aperture diaphragm (pinhole) made 404 microns. Images were recorded for a single confocal section in the middle of each cell. The fluorescence intensity of the NPs (arb. units) was determined using the Axio Examiner confocal microscope software (Carl Zeiss, Germany). Briefly, the cells in the field of view of the micrograph were enclosed by circles that limited the area of each cell or its individual compartments (LSM and LSM 510 2005).

The following parameters were studied:

- mean fluorescence intensity of NPs in a cell (arb. units);
- fluorescence intensity of NPs in nucleus, cytoplasm and in the beyond the cell.

Indices of tumor growth in vivo

- An absolute cell count (ACC) of EC cells was determined at day 7 after intraperitoneal inoculation of animal EC cells experimental and control groups according to the formula:

  $$\mathrm{ACC} = \mathrm{Vol} \times \mathrm{Conc},$$

  where Vol is the volume of ascitic fluid accumulated in it, Conc is the number of EC cells counted in the Goryaev chamber.
- Intensity growth of the EC (Int) was calculated by the formula:

  $$\mathrm{Int} = ((\mathrm{ACC\ (exp)}/\ \mathrm{ACC}(c)) \times 100\%,$$

  where ACC (exp) is an absolute cell count of EC cells in PC of the experimental group; ACC (c) is an absolute cell count of EC cells in PC of the control group.

Statistical analysis

The findings were statistically processed using the STATISTICA 8.0 software. Quantitative indices are presented as $X \pm m$, where X is the mean value, and m is the standard error of the mean. In the case of independent populations, the Mann–Whitney U test was used, and for the dependent sets, the Wilcoxon W test was applied. Differences were considered significant at $p < 0.05$.

Results and discussion

Incubation of EC cells with NPs for 1, 2, 3, and 4 h resulted in a slight decrease in the number of cells in all studied groups (Fig. 2a), although there was no statistically

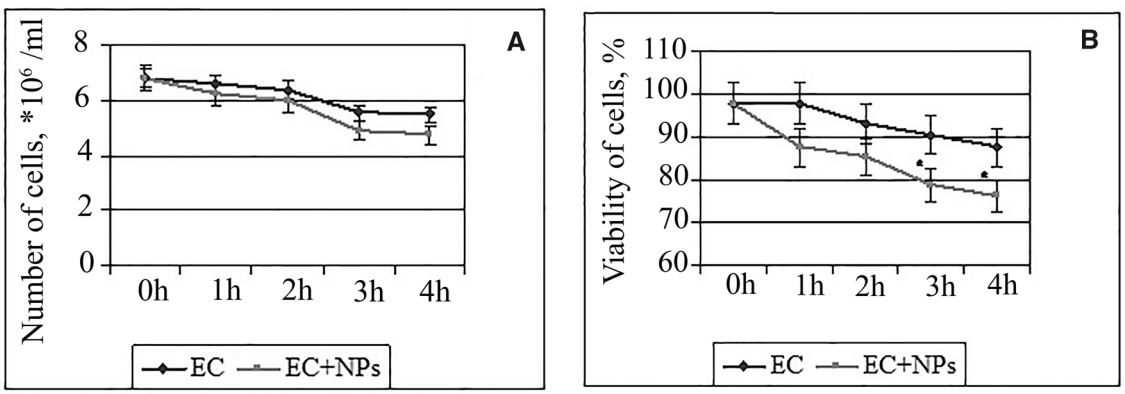

Fig. 2 Number of EC cells (**a**) and their viability (**b**) before and after incubation with nanoparticles. *Difference is statistically significant compared with similar indices of EC cells without incubation with NPs (control) ($p < 0.05$)

significant difference between them. After 3 h of incubation with NPs, the number of cells in the experimental group was 85.40 ± 4.22%, that was 12% less than initial values and 4% less than the control ones. The assessed by supravital trypan blue staining viability of EC cell was decreased after incubation with NPs and the control throughout the observation period (Fig. 2b), but only after 3 h of incubation, we noticed a 20% statistically significant decrease of this index both in comparison with baseline values and the control group ones. Thus, even at the first stage of attestation, it has been demonstrated that after 3 h of incubation of the EC cells with NPs, the studied parameters started their statistical and significant decrease.

The results of determining the fluorescence intensity of the EC cells are shown in Figs. 2 and 3. It has been demonstrated that the control samples, regardless of the incubation period, had an average fluorescence intensity of 15.33 ± 3.28 arb. units, which corresponds to the level of electronic noise in the detector (Fig. 3).

Confocal microscopy has shown the gradual penetration and accumulation of NPs in the EC cells during the time period under study (1–4 h) (Fig. 4). After 1 h of incubation, an increase in the mean fluorescence intensity (97.73 ± 10.13 arb. units) was detected for all the EC cells if compared to the control (15.33 ± 3.28 arb. units), which indicates the beginning of the accumulation of NPs inside the cells (Fig. 5).

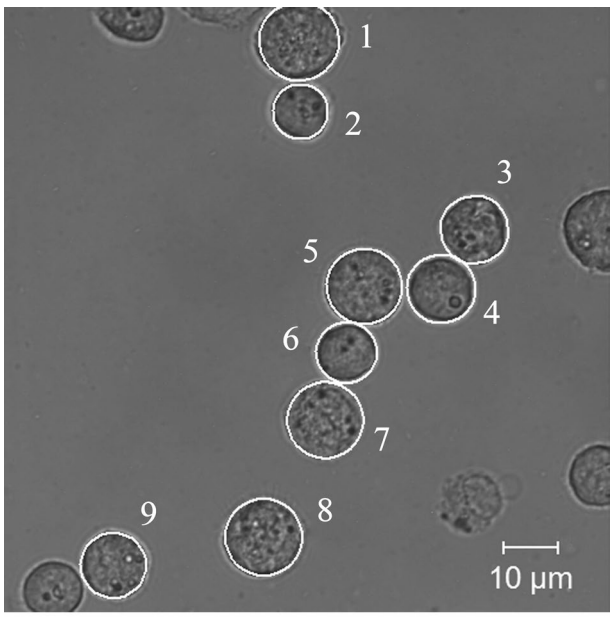

Image Region	1	2	3	4	5	6	7	8	9
Mean Intensity	12	17	21	17	10	15	16	17	13

Fig. 3 Confocal microscopy of EC cells without nanoparticles (control)

The mean fluorescence intensity of the total pool of EC cells after 2 h of incubation continued its rise (125.33 ± 20.28 arb. units) and reached a maximum by 3 h of incubation (177.27 ± 24.50 arb. units). At this time, we observed the appearance of single cells with a hyper-high level of fluorescence intensity (2220.50 ± 119.50 arb. units), the number of which did not exceed 5%. After 4 h of incubation, the mean fluorescence intensity of total cell population (cells with "medium-intensity" fluorescence) was somewhat decreased (137.75 ± 14.84 arb. units), while the number of single cells with hyper-high fluorescence remained at the same level (2172 ± 110.70 arb. units) like after 3-h incubation. Summarizing the data obtained, we can conclude that the most optimal time for the EC cell incubation with NPs was the time of 3 h.

At the next stage of the research, we analyzed the localization of NPs in different compartments of the EC cells after a 3-h incubation. The intracellular distribution of NPs was investigated by measuring the fluorescence intensity of NPs in the nucleus (1), cytoplasm (2), and in extracellular space (background fluorescence) (3). The obtained microscopic images of the cells after incubation with NPs demonstrated their diffuse accumulation inside the cytoplasm of cells, with the fluorescence values measured in the cytoplasm being higher compared to those obtained inside the nucleus or beyond the cells (Fig. 6a).

Moreover, it was shown that in nucleus of cells with "medium-intensity" fluorescence, there was no accumulation of NPs, in contrast to hyper-high-level fluorescence cells, wherein the fluorescence intensity of the nucleus was quite high (330 arb. units). In the control samples of the EC cells (Fig. 6b), the fluorescence intensity was within the range of 11–16 arb. units, regardless of the studied cell compartments, that testifies to the absence of intracellular accumulation of NPs.

One of the feasible mechanisms for the implementation of the cytotoxic effect of NPs based on orthovanadates of rare-earth elements is the ability to activate the cell prooxidant system (Averchenko et al. 2015), which is reflected in the changes of mitochondrial function. For this aim, the MTT assay was used. The method is based on the ability of living cell mitochondrial enzymes to convert soluble blue 3-[3.5 dimethylthiazol-2-yl]-2,5-diphenyl-2H-tetrazolium bromide—a yellow salt—into insoluble formazan having a purple color that crystallizes in the cytoplasm of a cell. The formazan can be dissolved with the help of an organic solvent (isopropanol). The intensity of formazan accumulation, estimated by means of spectrophotometric analysis, characterizes the degree of redox processes in the studied cells and is an indirect characteristic of the number of living cells.

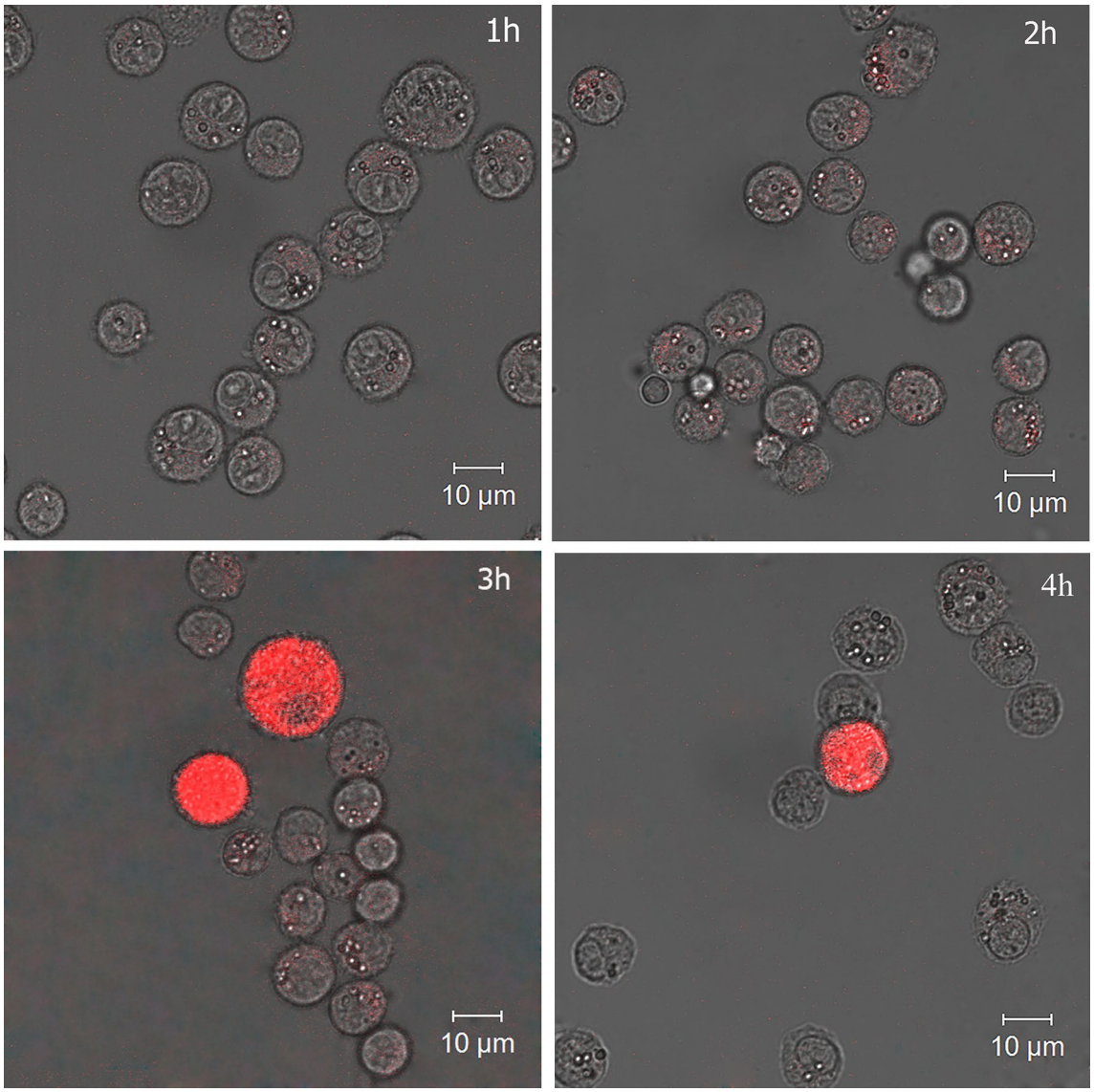

Fig. 4 Confocal microscopy of EC cells after incubation with nanoparticles for 1, 2, 3, and 4 h

The results of determining the metabolic activity of the EC cells after their incubation with NPs for various periods of time reflect the function of NADPH-dependent mitochondrial oxidoreductase enzymes. The tendency to a decrease in the MTT assay indices after the first hour of their incubation with NPs was established; however, during this period, we did not reveal statistically significant differences in comparison with the control (Fig. 7). The maximum disruption of functional activity of the EC cell mitochondria was noted after their 3-h incubation with NPs, as evidenced by a decrease in the formazan concentration by 30% during this observation period. Since the recovery of the tetrazolium dye depends mainly on the activity of cytosolic oxidoreductase enzymes, the data obtained explain the preferential localization of NPs in the cytoplasm as confirmed by confocal microscopy data (see Fig. 6).

Thus, the findings enable the suggestion that the used NPs contribute to a dysfunction of mitochondria due to their damage by free radicals, which is an early manifestation sign of a toxic effect of these NPs, and this dysfunction subsequently can lead to the death of tumor cells.

Many of the authors have shown that vanadium compounds, in particular, sodium orthovanadate can induce apoptosis of neuroblastoma cells (Tian et al. 2016), hepatocellular carcinoma (Wu et al. 2014) by inhibiting protein tyrosine phosphatases (Irving and Stoker 2017) or activation of tyrosine kinases (Korbecki et al. 2012).

Mitochondria are considered to be the main link integrating the various signals involved into implementation

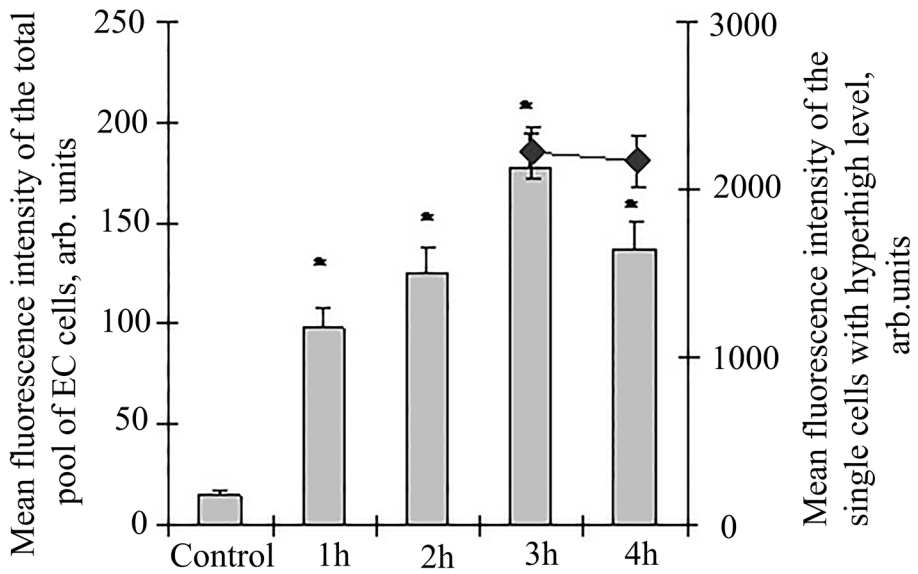

Fig. 5 Mean fluorescence intensity of total EC cell population (rectangular columns) and fluorescence of individual cells (blue marker) after incubation with nanoparticles for 1, 2, 3 and 4 h. *Difference is statistically significant compared with similar indices of EC cells without incubation with NPs (control) ($p < 0.05$)

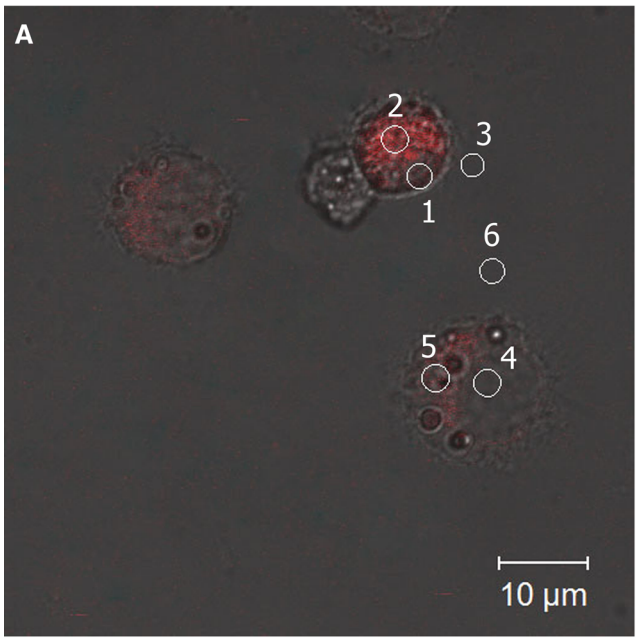

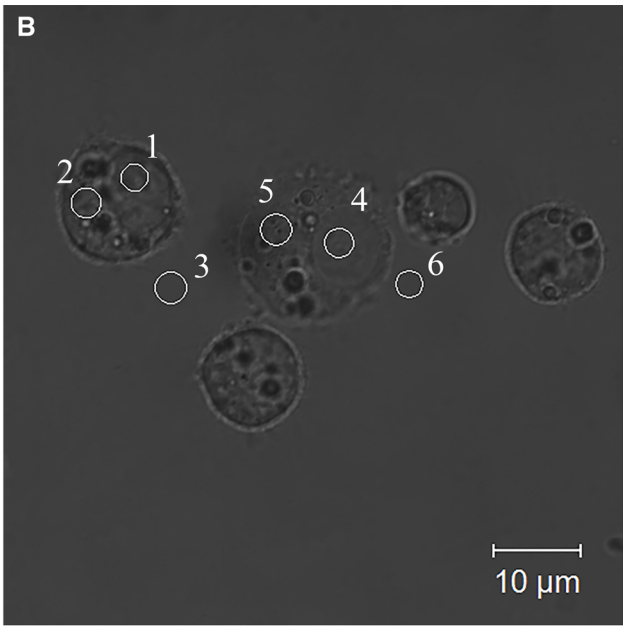

Marker location	nucleus		cytoplasm		beyond the cell	
Image Region	1	4	2	5	3	6
Mean Intensity	330	37	2220	177	29	24

Marker location	nucleus		cytoplasm		beyond the cell	
Image Region	1	4	2	5	3	6
Mean Intensity	13	11	15	14	16	13

Fig. 6 Localization of nanoparticles in EC cells (**a** after 3 h of incubation, **b** control). Circles denote the regions of interest of fluorescence (ROI), located in cell nucleus—1 and 4, in cytoplasm—2 and 5, beyond the cell (medium)—3 and 6

of apoptosis, i.e., programmed cell death. Simultaneous staining with Annexin V and PI reveals both the presence of necrotic cells and apoptosis. Annexin V in the presence of Ca^{2+} and Mg^{2+} ions interacts with phosphatidylserine, which at the early stages of apoptosis is translocated from an inner cell membrane to outer one. The cell membrane of

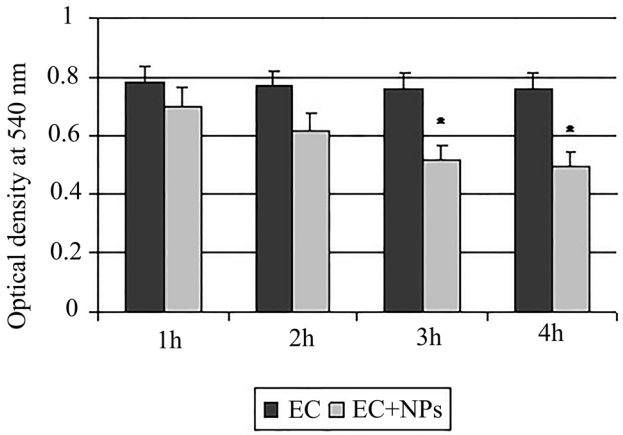

Fig. 7 Mitochondrial cell respiration of EC cells before and after incubation with nanoparticles. *Difference is statistically significant compared with similar indices of EC cells without incubation with NPs (control) ($p < 0.05$)

living cells is impermeable to propidium iodide (PI). However, with irreversible cell damage (necrosis), the propidium iodide passes through the cell membrane and interacts with the minor groove of deoxyribonucleic acid (DNA). Double staining with Annexin V and PI reveals the late stages of apoptosis.

It was established that throughout the observation period (1–4 h), the number of living cells (An^-/PI^-) in the control samples remained almost unchanged and made 90–94% (Fig. 8). At the same time, in the control, the percentage ratio of other studied populations (An^+/PI^-, An^+/PI^+, An^-/PI^+) was fairly stable, not changing significantly over time. The addition of NPs to the EC cells even after 1 h caused an increase in the amount of An^+/PI^- from 1.28 ± 0.1 to $6.11 \pm 0.3\%$ ($p < 0.05$), which indicated the re-arrangements in the composition of membranes under the NPs action. Further incubation of the cells with NPs (2–4 h) led to a gradual decrease in the proportion of living cells (An^-/PI^-) against the background of a rise in the percentage of the cells in states of late apoptosis (An^+/PI^+) and necrosis (An^-/PI^+) (Fig. 8), the maximum accumulation of which was noted 3 h after the incubation start. Besides, there were no statistically significant differences in the number of living cells and those being in a state of early, late apoptosis and necrosis after their incubation for 3 and 4 h.

The established fact of the presence of both apoptotic and necrotic changes in tumor cells after their incubation with NPs is important for the further development/inactivation of tumor process. If the cell death by apoptosis leads to the activation of phagocytosis without consequences for the body as an alteration and inflammation, then the consequence of necrosis is more potent inducer of inflammation than apoptosis (Sachet et al. 2017).

Activation of cell death along the path of apoptosis is believed to be one of the reasons of the failure of antitumor immune response of the body and the formation of immunological tolerance in malignant tumors (Fulda 2013). This leads to the conclusion that it is necessary to revise the treatment strategies and target them to switch the mechanism of tumor cell death from apoptotic to necrotic one. The above data indicate that the $GdYVO_4:Eu^{3+}$ nanoparticles used in this research are capable of solving this problem.

This assumption was tested in vivo by estimating the intensity of tumor development from the cells pretreated with NPs for different times (1–4 h) (Table 1). After 7 days of in vivo culturing of the EC cells of all the groups, the inhibitory effect of NPs on tumor growth was noted, and a statistically significant decrease in the intensity of growth rate of the EC was observed starting from the second hour of incubation. The maximum decrease in this index was found in the group with the developing tumor from the cells which had been pretreated with NPs for 3 h (41.80%) which indicated their pronounced antitumor effect.

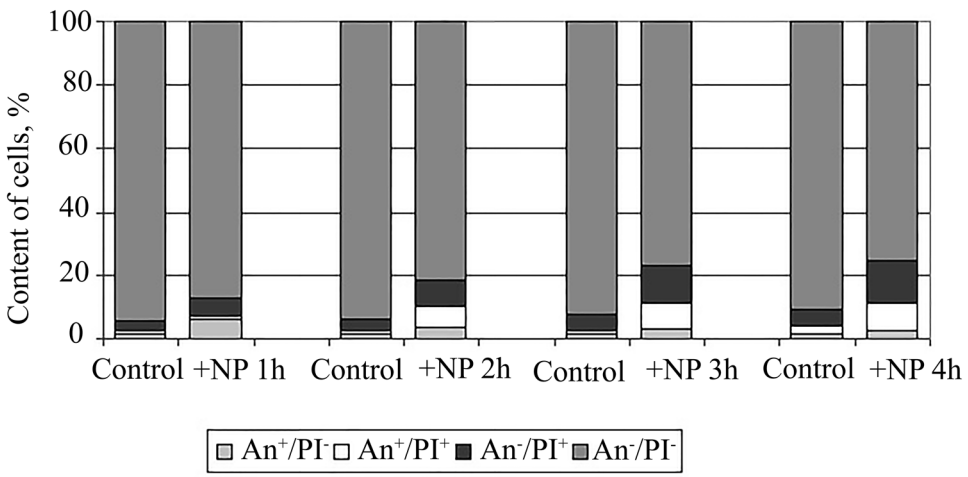

Fig. 8 Ratio of apoptotic/necrotic cells revealed with Annexin V/PI staining before and after incubation with nanoparticles

Table 1 Indices of tumor growth in vivo from cells pretreated with nanoparticles

Group	Volume of ascitic fluid, ml	Number of EC cells in PC, × 10^7	Absolute number of EC cells in PC, × 10^7	Intensity growth of the EC
Control (EC cells)	5.84 ± 0.77	9.54 ± 1.55	55.09 ± 7.56	100%
EC + NPs 1 h	4.4 ± 0.56	12.00 ± 2.03	51.14 ± 9.87	92.82
EC + NPs 2 h	4.26 ± 0.85	10.23 ± 1.38	43.57 ± 6.71	79.10
EC + NPs 3 h	3.08 ± 1.02	7.48 ± 2.09	23.03 ± 4.87*	41.80*
EC + NPs 4 h	2.62 ± 0.71	10.89 ± 1.90	27.58 ± 7.87*	49.06*

*Difference is statistically significant compared with similar indices of EC cells without incubation with NPs (control) ($p < 0.05$)

Indices of the EC growth rate induced by the cells after 3 and 4 h of pretreatment with NPs did not have statistically significant differences between themselves (41.80% and 49.06%). Based on the foregoing, the optimal incubation time of tumor cells with NPs, leading to a successful inhibition of tumor growth, can be considered a 3-h pretreatment. Effective implementation of antitumor effect of NPs based on orthovanadates of rare-earth elements activated by europium $GdYVO_4:Eu^{3+}$ implies their penetration and accumulation inside cells, impaired mitochondrial function with further induction of apoptotic and necrotic changes in tumor cells.

Conclusions

According to the confocal microscopy data, spherical nanoparticles based on orthovanadates of rare-earth elements activated by europium $GdYVO_4:Eu^{3+}$ were capable of penetrating almost all Ehrlich carcinoma cells; however, the intensity of their intracellular fluorescence was different. The presence of single cells with a high level of fluorescence intensity, the number of which did not exceed 5%, was noted. Penetration and accumulation of the NPS in the EC cells strongly depend on the incubation time. The fluorescence intensity of both the total pool of "medium-intensity" EC cells and single ones with hyper-high level reached a maximum by 3 h of incubating them with NPs. The most indicative disruption of functional activity of mitochondria of EC cells was found after their 3-h incubation with NPs, as evidenced by a reduction in the MTT assay indices by 30% compared with the control within this observation period. Incubation of EC cells with NPs for 3 h resulted in a significant rise in the percentage of cells in the states of late apoptosis (An^+/PI^+) and necrosis (An^-/PI^+) if compared to the control. The highest decrease in the intensity of tumor growth in vivo down to 41.80% was observed with a 3-h pretreatment of the EC cells by NPs. Summarizing the data obtained in vitro and in vivo, we can conclude that a 3-h pretreatment was the optimal incubation time for tumor cells with NPs, leading to successful identification and effective inhibition of tumor growth.

Compliance with ethical standards

Conflict of interest On behalf of all authors, the corresponding author states that there is no conflict of interest.

Research involving animal participants The experiments were carried out in accordance with the Law of Ukraine on the Protection of Animals Against Cruelty (2006), meeting the requirements of the Committee for Bioethics of the Institute, agreed with the statements of European Convention for the Protection of Vertebrate Animals used for Experimental and Other Scientific Purposes" (Strasbourg 1986).

References

Averchenko KA, Kavok NS, Klochkov VK, Sedyh OO, Yefimova SL, Malyukin YuV (2015) Effect of inorganic nanoparticles and organic complexes on their basis on free-radical processes in some model systems. Biopolym Cell 31(2):138–145. http://biopolymers.org.ua/doi/bc.0008D9

Dabros W, Nikiforuk A, Kordowiak AM (2004) The influence of bis(kojato)-oxovanadium (IV) on viability and proliferation of rat hepatoma cell line H 35-19. In: ELSO proceedings NICE, France abstract no. 653, p 299

Fulda S (2013) Regulation of cell death in cancer—possible implications for immunotherapy. Front Oncol 3:29. https://doi.org/10.3389/fonc.2013.00029

Goltsev AM, Safranchuk OV, Bondarovich MO, Ostankov MV, Babenko NN, Gayevskaya YuA, Chelombitko OV (2012) Methodical approaches to the stabilization of structural and functional states of cryopreserved cells of Ehrlich carcinoma. Rep Natl Acad Sci Ukraine 8:115–122 **(Ukrainian)**

Goltsev AN, Babenko NN, Gayevskaya YuA, Bondarovich NA, Ostankov MV, Chelombitko OV, Dubrava TG, Klochkov VK, Kavok NS, Malyukin YuV (2013) Capability of orthovanadate-based nanoparticles to in vitro identification and in vivo inhibition of cancer stem cells. Nanosyst Nanomater Nanotechnol 11(4):729–739 **(Ukrainian)**

Goltsev AN, Babenko NN, Gaevskaya YA, Chelombitko OV, Dubrava TG, Bondarovich NA, Ostankov MV, Klochkov VK, Kavok NS, Vinnik YuV, Malyukin YV (2015) Application of nanoparticles based on rare-earth orthovanadates to inactivate Ehrlich carcinoma growth. Biotechnol Acta 8(4):113–121. https://doi.org/10.15407/biotech8.04.113

Goltsev AN, Malyukin YV, Dubrava TG, Babenko NN, Gaevskaya YA, Chelombytko OV, Bondarovich NA, Ostankova LV, Dimitrov AY, Klochkov VK, Kavok NS (2016) Nanocomposites specifically penetrate and inhibit tumor cells. Mat-wiss u Werkstofftech 47(2–3):156–164. https://doi.org/10.1002/mawe.201600457

Goltsev AN, Babenko NN, Gaevskaya YA, Bondarovich NA, Dubrava TG, Ostankov MV, Chelombitko OV, Malyukin YV, Klochkov VK, Kavok NS (2017) Nanotechniques inactivate cancer stem cells. Nanoscale Res Lett 12(1):415. https://doi.org/10.1186/s11671-017-2175-9

Holtsev AM, Safranchuk OV, Bondarovich MO, Ostankov MV (2011) Change in cryolability of tumour stem cells depending on adenocarcinoma growth phase. Fiziol Zh 57(4):68–76 **(Ukrainian)**

Irving E, Stoker AW (2017) Vanadium Compounds as PTP Inhibitors. Molecules 22(12):E2269. https://doi.org/10.3390/molecules22122269

Klochkov VK (2009) Aqueous colloid solutions of nanoluminophores $nReVO_4:Eu^{3+}$ (Re = Y, Gd, La). Mater Sci Nanostruct 2:3–8 **(Ukrainian)**

Klochkov V, Kavok N, Grygorova G, Sedyh O, Malyukin Y (2013) Size and shape influence of luminescent orthovanadate nanoparticles on their accumulation in nuclear compartments of rat hepatocytes. Mater Sci Eng C 33(5):2708–2712. https://doi.org/10.1016/j.msec.2013.02.046

Korbecki J, Baranowska-Bosiacka I, Gutowska I, Chlubek D (2012) Biochemical and medical importance of vanadium compounds. Acta Biochim Pol 59(2):195–200

Kordowiak AM, Klein A, Goc A, Dabroś W (2007) Comparison of the effect of VOSO4, Na3VO4 and NaVO3 on proliferation, viability and morphology of H35-19 rat hepatoma cell line. Pol J Pathol 58(1):51–57

LSM 510 and LSM 510 META (2005) Laser scanning microscopes. Operating manual. Release 3.2

Molinuevo MS, Barrio DA, Cortizo AM, Etcheverry SB (2004) Antitumoral properties of two new vanadyl (IV) complexes in osteoblasts in culture: role of apoptosis and oxidative stress. Cancer Chemother Pharmacol 53(2):163–172

Ozaslan M, Karagoz ID, Kilic IH, Guldur ME (2011) Ehrlich ascites carcinoma. Afr J Biotechnol 10(13):2375–2378

Rodríguez-Mercado JJ, Mateos-Nava RA, Altamirano-Lozano MA (2011) DNA damage induction in human cells exposed to vanadium oxides in vitro. Toxicol In Vitro 25:1996–2002. https://doi.org/10.1016/j.tiv.2011.07.009

Rozzo C, Sanna D, Garribba E, Serra M, Cantara A, Palmieri G, Pisano M (2017) Antitumoral effect of vanadium compounds in malignant melanoma cell lines. J Inorg Biochem 174:14–24. https://doi.org/10.1016/j.jinorgbio.2017.05.010

Sachet M, Liang YY, Oehler R (2017) The immune response to secondary necrotic cells. Apoptosis 22(10):1189–1204. https://doi.org/10.1007/s10495-017-1413-z

Tian X, Fan J, Hou W, Bai S, Ao Q, Tong H (2016) Sodium orthovanadate induces the apoptosis of SH-SY5Y cells by inhibiting PIWIL2. Mol Med Rep 13(1):874–880. https://doi.org/10.3892/mmr.2015.4616

Wu Y, Ma Y, Xu Z, Wang D, Zhao B, Pan H, Wang J, Xu D, Zhao X, Pan S, Liu L, Dai W, Jiang H (2014) Sodium orthovanadate inhibits growth of human hepatocellular carcinoma cells in vitro and in an orthotopic model in vivo. Cancer Lett 351(1):108–116. https://doi.org/10.1016/j.canlet.2014.05.018